

UNIVERSIDAD DE CONCEPCIÓN



CENTRO DE INVESTIGACIÓN EN  
INGENIERÍA MATEMÁTICA (CI<sup>2</sup>MA)



Simulation of the secondary settling process with reliable  
numerical methods

RAIMUND BÜRGER, STEFAN DIEHL,  
SEBASTIAN FARÅS, INGMAR NOPENS

PREPRINT 2011-14

SERIE DE PRE-PUBLICACIONES



# Simulation of the secondary settling process with reliable numerical methods

R. Bürger\*, S. Diehl\*\*, S. Farås\*\*\*° and I. Nopens\*\*\*

\*CI<sup>2</sup>MA and Departamento de Ingeniería Matemática, Facultad de Ciencias Físicas y Matemáticas, Universidad de Concepción, Casilla 160-C, Concepción, Chile. (E-mail: rburger@ing-mat.udec.cl)

\*\*Centre for Mathematical Sciences, Lund University, P.O. Box 118, SE-221 00 Lund, Sweden. (E-mail: diehl@maths.lth.se; faras@maths.lth.se)

\*\*\*BIOMATH, Department of Applied Mathematics, Biometrics and Process Control, Coupure Links 653, 9000 Gent, Belgium. (E-mail: ingmar.nopens@ugent.be)

°Corresponding author. The authors are placed in alphabetical order

## Abstract

A consistent model for the settling-compression-dispersion process in the secondary settling tank (SST) can be expressed as a partial differential equation (PDE). Reliable numerical methods for simulation produce approximate solutions that converge to the physically relevant solution of the PDE as the discretization is refined. We focus on two methods and assess their performance via simulations for two scenarios. One method is provably convergent and is used as a reference method. The other method is less efficient in reducing numerical errors, but faster and more easily implemented.

## Keywords

Sedimentation, clarifier, conservation law, partial differential equation, numerical flux

## INTRODUCTION

The sedimentation process in the secondary settling tank (SST) is still a challenge in modelling the full-scale operation of wastewater treatment plants (WWTPs). In the modelling of the activated sludge process, biological reactors have traditionally received more attention than the SSTs. This was mainly due to the wish to predict the effluent quality and the role of the SST model was to create a reasonable sludge balance. The main commercial simulators, however, do not provide reliable simulation methods in the sense that there is no guarantee that the simulations satisfy fundamental physical properties. From a practical point of view, current SST models tend to fail under wet weather conditions where a significant amount of sludge mass is recycled within the plant. Recent efforts to improve SST models are presented by Verdickt et al. (2005), Nocoñ (2006), Plósz et al. (2007, 2011), De Clercq et al. (2008), Abusam and Keesman (2009), David et al. (2009a, 2009b). From a consistent modelling point of view, the commonly used simulation models have no proved connection to the underlying physical principles. These principles can be captured by a mathematical model on integral form or as a partial differential equation (PDE). The model equation cannot be expected to have a closed-form solution. Hence, a numerical method is needed. The core of the paper by Bürger et al. (2011a) is that such a method should be derived from the model equation and produce approximate solutions that converge to the exact solution as the discretization is refined. They propose a one-dimensional (1D) model that captures most of the phenomena addressed by previously published 1D models: hindered settling, compression at high concentrations and dispersion due to turbulence. As a reference method, denoted Method EO, we use the robust numerical method for such a PDE (without dispersion) by Bürger et al. (2005), which is the only publication with a convergence proof. This method was also used by De Clercq et al. (2008). A simplified and more easily implemented method – here called Method G – is launched by Bürger et al. (2011b). The purpose of the current work is to compare these two methods regarding accuracy and required CPU times.

## THE MODEL ON PDE FORM

Suppose that the sludge concentration  $C$  is horizontally homogenous. Then it can be treated as a function of depth  $z$  and time  $t$  only. Let  $A$  be the (constant) cross-sectional area of the tank and  $Q_f$  and  $C_f$  the volumetric flow rate and concentration of the feed inlet, respectively. The conservation of mass yields a model equation in integral form (see (1) below), which is equivalent to the following PDE, interpreted in the weak sense:

$$\frac{\partial C}{\partial t} + \frac{\partial}{\partial z} F(C, z, t) = \frac{\partial}{\partial z} \left( (\gamma(z) d_{\text{comp}}(C) + d_{\text{disp}}(z, Q_f)) \frac{\partial C}{\partial z} \right) + \frac{Q_f(t) C_f(t)}{A} \delta(z).$$

Here,  $\gamma(z)$  is a characteristic function which is equal to 1 inside the tank and zero outside. The last term is a point source where  $\delta$  is the Dirac delta distribution. Dispersion (turbulence), e.g. near the feed inlet, is modelled by  $d_{\text{disp}}$  and compression by  $d_{\text{comp}}$ . The latter function is assumed to be nonzero for concentrations above a critical concentration  $C_c$  at which the flocs begin to form a compressible network. If  $f_b$  denotes the batch flux function (the product of the concentration and the Kynch hindered settling velocity), then the flux function  $F$  depends discontinuously on  $z$  in the following way:

$$F(C, z, t) = \begin{cases} -Q_e(t)C/A & \text{for } z < -H & \text{(Effluent zone)} \\ f_b(C) - Q_e(t)C/A & \text{for } -H < z < 0 & \text{(Clarification zone)} \\ f_b(C) + Q_u(t)C/A & \text{for } 0 < z < B & \text{(Thickening zone)} \\ Q_u(t)C/A & \text{for } z > B & \text{(Underflow zone),} \end{cases}$$

where  $H$  is the height of the clarification zone and  $B$  is the depth of the thickening zone. The volumetric flow rates in the effluent and the underflow are given by  $Q_e$  and  $Q_u$ , respectively.

## THE MODEL ON INTEGRAL FORM AND NUMERICAL METHODS

The derivation of a reliable numerical method starts from the integral form of the conservation law:

$$\frac{d}{dt} \int_{z_1}^{z_2} C(z, t) dz = \Phi|_{z=z_1} - \Phi|_{z=z_2} + \frac{1}{A} \int_{z_1}^{z_2} Q_f(t) C_f(t) \delta(z) dz, \quad (1)$$

where  $(z_1, z_2)$  is an arbitrary interval of the  $z$ -axis (a layer in the method) and the flux  $\Phi$  is

$$\Phi \left( C, \frac{\partial C}{\partial z}, z, t \right) = F(C, z, t) - (\gamma(z) d_{\text{comp}}(C) + d_{\text{disp}}(z, Q_f)) \frac{\partial C}{\partial z}.$$

The  $z$ -axis is divided into a finite number of layers and a method-of-lines formulation of the numerical method is possible, i.e. a system of ordinary differential equations. This system is discretized in time with explicit Euler steps constrained by a CFL condition to assure stability. In the spatial discretization,  $F$  demands some extra care and this is precisely where the most important difference between Method G and Method EO occurs. The short discussion here is therefore focused on this part and we refer to Bürger et al. (2005, 2011b) for further details. Let  $C_j(t)$  and  $C_{j+1}(t)$  denote the average concentrations at time  $t$  in two neighbouring layers  $j$  and  $j+1$  within the SST. Furthermore, if  $z_j$  is the depth of the boundary between the two layers, then  $F_j^{\text{num}}$  denotes the numerical flux that approximates  $F$  across  $z_j$ . There are several reasonable techniques to

compute  $F_j^{\text{num}}$  (LeVeque, 2002). We use here the formulas by Engquist and Osher (1981) and Godunov (1959). Each of these formulas can be applied in two consistent ways. For simplicity of description, consider only the thickening zone ( $0 < z < B$ ) (the clarification-zone case is analogous). The flux in the thickening zone  $f$  is given by the superposition of the nonlinear function  $f_b$  and a linear term due to the downward bulk flow:  $f(C, t) = f_b(C) + Q_u(t)C/A$ . One way is to apply the Engquist-Osher (or Godunov) formula directly on the total flux  $f$ . This was done with the Engquist-Osher formula by Bürger et al. (2005), whereas Diehl and Jeppsson (1998) used the Godunov formula. Another way is to apply the chosen formula on the batch flux  $f_b$  alone, while the linear term is discretized in an upwind fashion by replacing  $Q_u C/A$  with  $Q_u C_j/A$ . This leads to a simpler implementation but at the cost of extra numerical viscosity. We have thus four possible ways of computing the numerical flux  $F_j^{\text{num}}$ . In light of the convergence results by Bürger et al. (2005), we choose as the numerical flux in Method EO the Engquist-Osher formula on  $f$ :

$$F_j^{\text{num, EO}} = \frac{1}{2} \left( f(C_j, t) + f(C_{j+1}, t) - \int_{C_j}^{C_{j+1}} \left| \frac{\partial f}{\partial C} (C, t) \right| dC \right).$$

In Method G, we choose instead the numerical flux

$$F_j^{\text{num, G}} = \frac{Q_u(t)}{A} C_j + \begin{cases} \min_{C_j \leq C \leq C_{j+1}} f_b(C) & \text{for } C_j < C_{j+1} \\ \max_{C_{j+1} \leq C \leq C_j} f_b(C) & \text{for } C_j \geq C_{j+1}, \end{cases}$$

where the bracketed term is the Godunov formula applied to  $f_b$ . Jeppsson and Diehl (1996) have demonstrated the advantages of the Godunov formula compared with the minimum-flux formula by Vitasovic (1989) in the well-known method by Takács et al. (1991). Another example of failure of the Vitasovic-Takács formula is provided by Bürger et al. (2011a). Our algorithm for the implementation of Method G (Bürger et al., 2011b) has the feature that it can be seen as an extension of the Vitasovic-Takács formula.

## SIMULATIONS

In order to compare Method G with EO properly, it is necessary to use the same division of the  $z$ -axis for both. Therefore, we choose  $H = 1$ ,  $B = 3$  and let the number of internal layers (within the SST) be  $N = 10 \cdot 3^p$  for  $p = 0, 1, \dots, 5$ . The comparison is performed by simulations of two scenarios starting at the same steady state (computed with Method EO). In both scenarios,  $A = 400 \text{ m}^2$  is used and the constitutive functions  $f_b$  and  $d_{\text{comp}}$  are chosen according to De Clercq et al. (2008) but with some changes of the parameters:

$$f_b(C) = v_0 C e^{-rC} \quad \text{and} \quad d_{\text{comp}}(C) = \begin{cases} \frac{\rho_s \sigma_0 f_b(C)}{\Delta \rho g C (C - C_c + k)} & \text{for } C \geq C_c \\ 0 & \text{for } C < C_c, \end{cases}$$

where  $v_0 = 3.47 \text{ m/h}$ ,  $r = 0.37 \text{ m}^3/\text{kg}$ ,  $\sigma_0 = 4.00 \text{ Pa}$  and  $k = 4.00 \text{ kg/m}^3$ . The density of the solids is  $\rho_s = 1050 \text{ kg/m}^3$ , the density difference between the solids and water is  $\Delta \rho = 52 \text{ kg/m}^3$ , the acceleration of gravity is  $g = 9.81 \text{ m/s}^2$  and the critical concentration is  $C_c = 6.00 \text{ kg/m}^3$ . The third constitutive function  $d_{\text{disp}}$  is set to be increasing with the feed flow rate  $Q_f$  and assumed to be

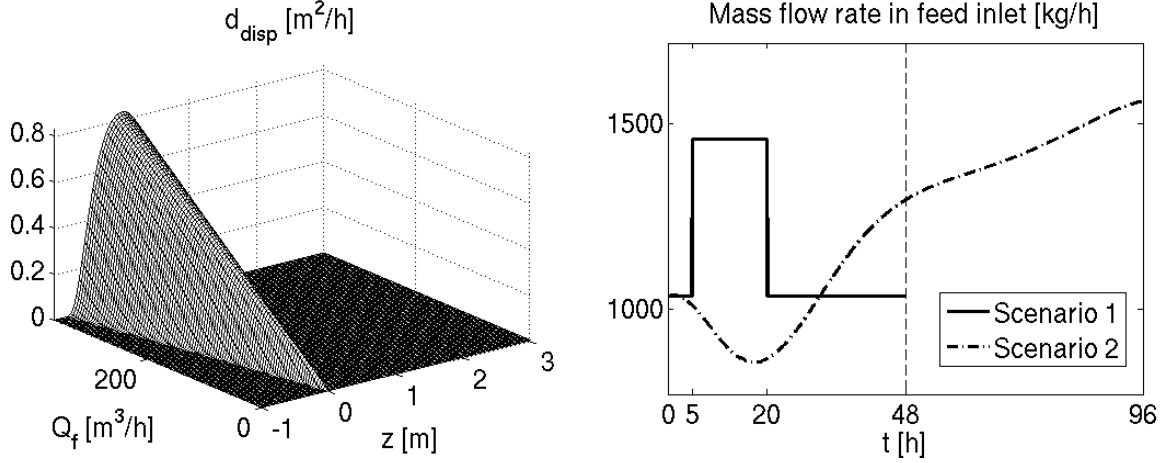


**Figure 1:** Graphs of functions used in the simulations of Scenario 1 and 2. **Left:** The dispersion coefficient  $d_{\text{disp}}(z, Q_f)$ . **Right:** The mass flow rate  $Q_f(t)C_f(t)$  in the feed inlet.

nonzero around the inlet only:

$$d_{\text{disp}}(z, Q_f) = \begin{cases} \alpha_1 Q_f \exp\left(\frac{-z^2 / (\alpha_2 Q_f)^2}{1 - |z| / (\alpha_2 Q_f)}\right) & \text{for } |z| < \alpha_2 Q_f \\ 0 & \text{for } |z| \geq \alpha_2 Q_f \end{cases}$$

where  $\alpha_1 = 0.0023 \text{ m}^{-1}$  and  $\alpha_2 = 0.0025 \text{ h/m}^2$ , see Figure 1 (left).

To illustrate the convergence and define suitable error measures, a reference solution was generated with Method EO using  $N = 2430$  ( $p = 5$ ) for each scenario. Subsequently, solutions for  $N = 10, 30, 90, 270$  and  $810$  were produced with both methods. The scenarios are constructed to demonstrate and compare the two methods and to show their robustness. Therefore, extreme variations in the concentrations and flow rates have been imposed.

### Scenario 1

We start in a steady state with the feed flow rate  $Q_f = 230 \text{ m}^3/\text{h}$ , the feed concentration  $C_f = 4.5 \text{ kg/m}^3$ , the underflow rate  $Q_u = 100 \text{ m}^3/\text{h}$  and with a sludge blanket in the thickening zone. At  $t = 5 \text{ h}$ , we impose a step increase in the mass flow rate in the feed inlet constructed by changing  $Q_f$  to  $360 \text{ m}^3/\text{h}$ , decreasing  $C_f$  by 10% and keeping the underflow rate constant, see Figure 1 (right). At  $t = 20 \text{ h}$  all variables are returned to their initial values. The total simulation time is  $T = 48 \text{ h}$ .

### Scenario 2

The same initial state as in Scenario 1 is used. Throughout the simulation, the underflow and effluent flow rates are kept proportional to the feed flow rate:  $Q_u = \beta Q_f$  and  $Q_e = (1 - \beta)Q_f$  where  $\beta = 10/23$  (i.e. the same ratio as in the initial state). The mass flow rate in the feed inlet is changed according to Figure 1 (right) with the feed flow rate  $Q_f$  oscillating around its initial value with period 24 h and amplitude  $50 \text{ m}^3/\text{h}$ . The total simulation time is  $T = 96 \text{ h}$ .

### System specification and implementation details

The implementations were done in Matlab mex-files (written in C) and were run on a Unix platform (Ubuntu 11.01) using an Intel Core i7 processor (2.8 GHz) with a single thread only.

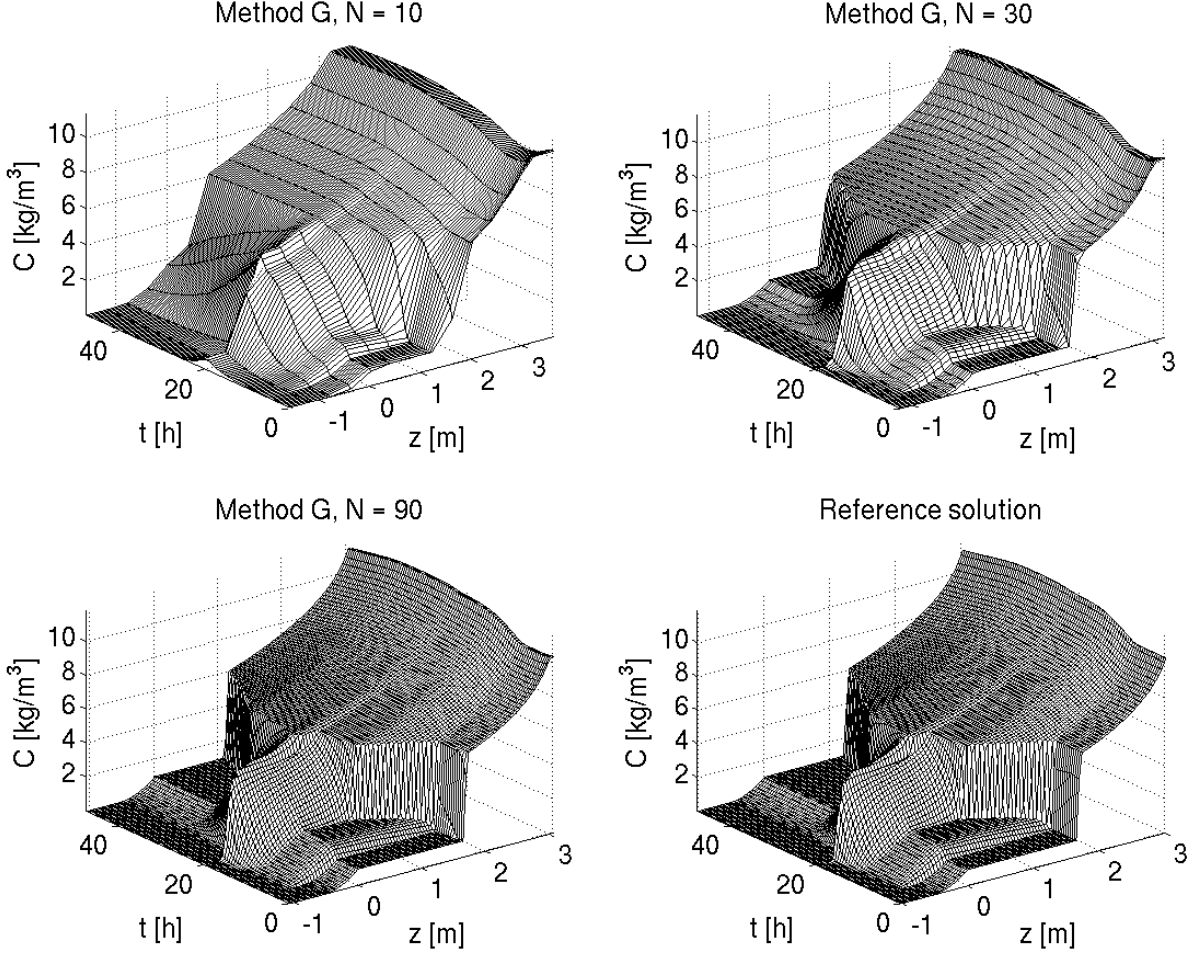


**Figure 2:** Four approximate solutions for Scenario 1. The reference solution in the lower right plot is computed with Method EO for  $N = 2430$  internal layers, while the others are computed with Method G for 10, 30 and 90 internal layers.

## RESULTS

A selection of numerical solutions generated by Method G for Scenario 1 is presented in Figure 2. The corresponding reference solution is shown in the lower right figure. It is evident how the solution for  $N=10$  layers deviates from the reference solution, but as the number of layers increases the solutions clearly converge. The solutions for Scenario 2 are presented in a slightly different way in Figure 3.

Motivated by the convergence analysis for Method EO in Bürger et al. (2005), it is reasonable to assume that the reference solutions for  $N = 2430$  internal layers are the ones closest to the true solution for the given input data in each scenario. In order to quantify the performance of Method G compared with Method EO, the following error measures are used in Table 1:

$$e_c = \frac{\int_0^T \int_{-H}^B |C^N(z, t) - C^{\text{ref}}(z, t)| dz dt}{\int_0^T \int_{-H}^B C^{\text{ref}}(z, t) dz dt} \quad \text{and} \quad e_m = \frac{\int_0^T |m^N(t) - m^{\text{ref}}(t)| dt}{\int_0^T m^{\text{ref}}(t) dt}.$$

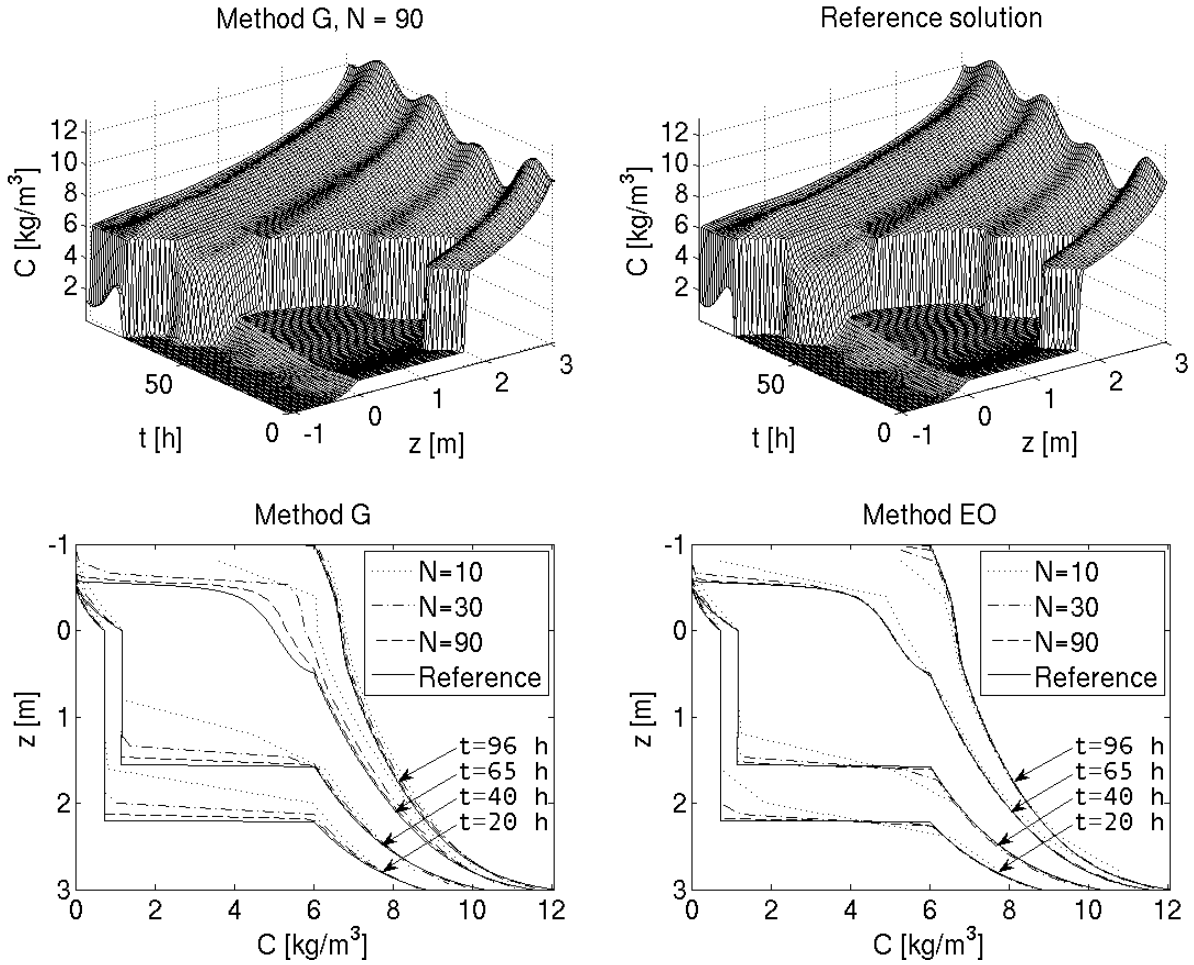


**Figure 3:** Scenario 2. **Top:** A simulation produced with Method G for  $N = 90$  internal layers (left) and the reference solution (right). **Bottom:** Concentration profiles from the solutions produced with Method G (left) and Method EO (right) for  $N = 10, 30$  and  $90$  internal layers.

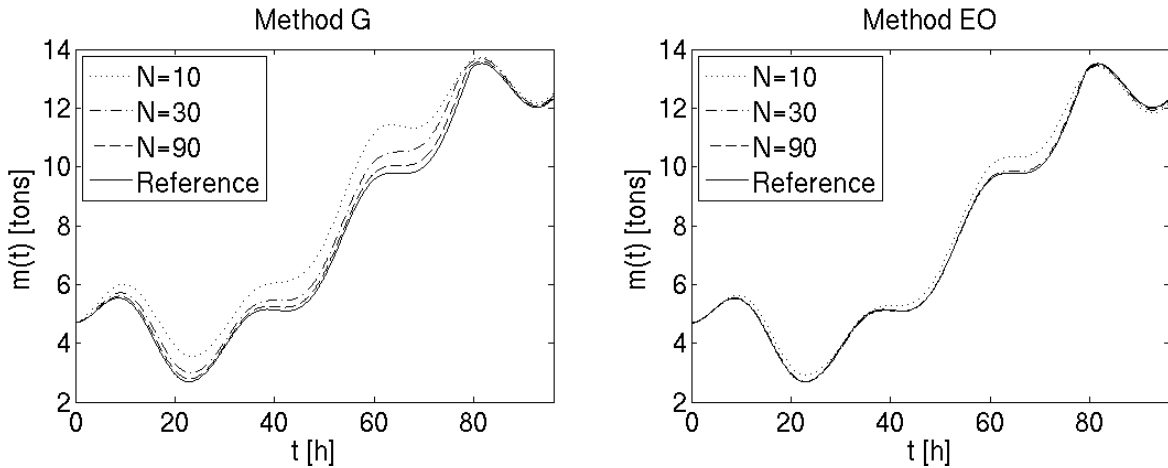


**Figure 4:** Masses for Scenario 2. The mass  $m^N(t)$  for different number of internal layers are plotted together with  $m^{\text{ref}}(t)$ . **Left:** The underlying solutions are produced with Method G. **Right:** The underlying solutions are produced with Method EO.

In the relative error  $e_c$ ,  $C^N$  is a piecewise constant representation of the solution generated over  $N$  internal layers by any of the two methods and  $C^{\text{ref}}$  is the reference solution restricted to the same grid. In the relative mass error  $e_m$ ,  $m^N(t)$  and  $m^{\text{ref}}(t)$  are the masses in the SST at time  $t$  derived from  $C^N$  and  $C^{\text{ref}}$ , respectively. Figure 4 shows the time variations for the masses in Scenario 2.

From the columns containing the CPU times in Table 1, it is seen that Method G is faster than Method EO for any fixed  $N$ . However, this comes at the cost of less accurate solutions, which is clear from both error measures. On the other hand, comparing the required CPU times to reach an error below a certain threshold value reveals that Method EO is more efficient for both scenarios. This point is emphasized in Figure 5, where  $e_c$  is plotted against the corresponding CPU time for each simulation.

**Table 1:** Errors and CPU times for Method G and Method EO applied to Scenario 1 and Scenario 2.

	Scenario 1			Scenario 2			
	$N$	$e_c$ [-]	$e_m$ [-]	CPU time [s]	$e_c$ [-]	$e_m$ [-]	CPU time [s]
Method G	10	$1.68 \cdot 10^{-1}$	$1.30 \cdot 10^{-1}$	$3.13 \cdot 10^{-3}$	$1.29 \cdot 10^{-1}$	$1.09 \cdot 10^{-1}$	$3.15 \cdot 10^{-3}$
	30	$8.30 \cdot 10^{-2}$	$7.26 \cdot 10^{-2}$	$1.97 \cdot 10^{-2}$	$5.43 \cdot 10^{-2}$	$4.71 \cdot 10^{-2}$	$4.37 \cdot 10^{-2}$
	90	$3.06 \cdot 10^{-2}$	$2.72 \cdot 10^{-2}$	$4.06 \cdot 10^{-1}$	$1.98 \cdot 10^{-2}$	$1.73 \cdot 10^{-2}$	$8.49 \cdot 10^{-1}$
	270	$1.04 \cdot 10^{-2}$	$9.36 \cdot 10^{-3}$	$9.63 \cdot 10^0$	$6.85 \cdot 10^{-3}$	$6.07 \cdot 10^{-3}$	$2.03 \cdot 10^1$
	810	$3.49 \cdot 10^{-3}$	$3.24 \cdot 10^{-3}$	$2.53 \cdot 10^2$	$2.35 \cdot 10^{-3}$	$2.17 \cdot 10^{-3}$	$5.34 \cdot 10^2$
Method EO	10	$5.13 \cdot 10^{-2}$	$4.03 \cdot 10^{-2}$	$4.28 \cdot 10^{-3}$	$4.62 \cdot 10^{-2}$	$3.21 \cdot 10^{-2}$	$1.42 \cdot 10^{-2}$
	30	$1.56 \cdot 10^{-2}$	$7.61 \cdot 10^{-3}$	$3.55 \cdot 10^{-2}$	$1.39 \cdot 10^{-2}$	$6.27 \cdot 10^{-3}$	$1.07 \cdot 10^{-1}$
	90	$5.36 \cdot 10^{-3}$	$1.06 \cdot 10^{-3}$	$9.75 \cdot 10^{-1}$	$5.18 \cdot 10^{-3}$	$2.48 \cdot 10^{-3}$	$2.04 \cdot 10^0$
	270	$1.69 \cdot 10^{-3}$	$8.00 \cdot 10^{-4}$	$2.43 \cdot 10^1$	$1.84 \cdot 10^{-3}$	$1.23 \cdot 10^{-3}$	$5.01 \cdot 10^1$
	810	$4.60 \cdot 10^{-4}$	$3.04 \cdot 10^{-4}$	$6.71 \cdot 10^2$	$4.89 \cdot 10^{-4}$	$3.46 \cdot 10^{-4}$	$1.34 \cdot 10^3$

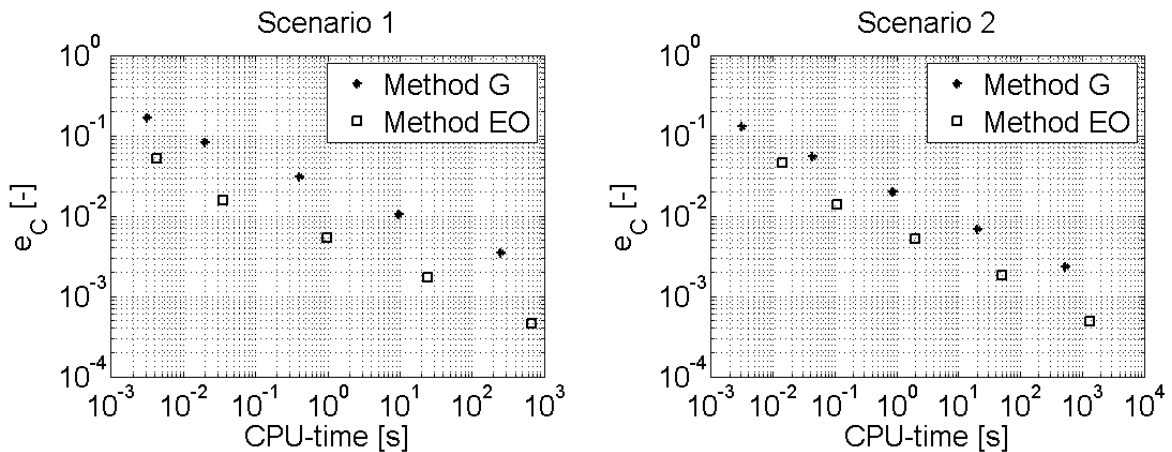


**Figure 5:** The error  $e_c$  versus CPU time for Scenario 1 (left) and Scenario 2 (right).

## CONCLUSIONS

We recommend the use of reliable numerical methods for simulation. The number of layers  $N$  should only be a parameter that controls the quality of approximation of the exact solution of the model PDE. The number of layers is not a parameter to be adjusted to a particular physical reality. This paper illustrates how recent results of numerical analysis can be used for the practical application to the simulation of SSTs. Applied mathematical research has led to several alternative methods, represented here by Method G and Method EO, which are both sound in the sense that they converge to the solution of the PDE. The choice of method to be implemented in a simulator is subject to several competing principles. As our results show, for a given value of  $N$ , Method G produces a numerical solution faster than Method EO, but the value of this advantage is questionable since Method EO is more efficient than Method G in reducing the numerical error. In other words, the disadvantage of larger CPU times associated with Method EO is more than compensated by the gain in quality of numerical solutions if compared with Method G. This quality difference is a result of the application of the numerical flux formula to the total flux and the batch settling flux, respectively, rather than the choice of numerical flux formula (Engquist-Osher or Godunov). An aspect that speaks in favour of Method G is its ease of implementation.

## REFERENCES

- Abusam A. and Keesman K. J. (2009). Dynamic modeling of sludge compaction and consolidation processes in wastewater secondary settling tanks. *Water Environ. Res.* 81(1), 51–56.
- Bürger R., Karlsen K. H. and Towers J. D. (2005). A model of continuous sedimentation of flocculated suspensions in clarifier-thickener units, *SIAM J. Appl. Math.* 65, 882–940.
- Bürger R., Diehl S. and Nopens, I. (2011a). A consistent modelling methodology for secondary settling tanks in wastewater treatment. *Water Research*, 45(6), 2247–2260.
- Bürger R., Diehl S., Farás S., Nopens I. and Torfs E. (2011b). A consistent modelling methodology for secondary settling tanks. Part 2: Numerical methods. (in preparation).
- David R., Saucez P., Vasel J.-L. and Vande Wouwer A. (2009a). Modeling and numerical simulation of secondary settlers: A method of lines strategy. *Water Res.* 43(2), 319–330.
- David R., Vasel J.-L. and Vande Wouwer A. (2009b). Settler dynamic modeling and MATLAB simulation of the activated sludge process. *Chem. Eng. J.* 146, 174–183.
- Diehl S. and Jeppsson U. (1998). A model of the settler coupled to the biological reactor. *Water Res.* 32(2), 331–342.
- De Clercq J., Nopens I., Defrancq J. and Vanrolleghem P. A. (2008). Extending and calibrating a mechanistic hindered and compression settling model for activated sludge using in-depth batch experiments. *Water Res.* 42, 781–791.
- Engquist B. and Osher S. (1981). One-sided difference approximations for nonlinear conservation laws. *Math. Comp.* 36, 321–351.
- Godunov S. K. (1959). A finite difference method for the numerical computations of discontinuous solutions of the equations of fluid dynamics, *Mat. Sb.* 47, 271–306 (in Russian).
- Jeppsson U. and Diehl S. (1996). An evaluation of a dynamic model of the secondary clarifier. *Water Sci. Tech.* 34(5–6), 19–26.
- LeVeque R. J. (2002). *Finite Volume Methods for Hyperbolic Problems*. Cambridge University Press.
- Nocoń W. (2006). Mathematical modelling of distributed feed in continuous sedimentation. *Simulat. Model. Pract. Theor.* 14(5), 493–505.
- Plósz B. Gy., Weiss M., Printemps C., Essemiani K., and Meinhold J. (2007). One-dimensional modelling of the secondary clarifier — factors affecting simulation in the clarification zone and the assessment of the thickening flow dependence. *Water Res.* 41(15), 3359–3371.
- Plósz B. Gy., Nopens I., De Clercq J., Benedetti L. and Vanrolleghem P. A. (2011). Shall we upgrade one-dimensional secondary settler models in WWTP simulators? Yes. *Water Sci. Tech.* 63(8), 1726–1738.
- Takács I., Patry G. G. and Nolasco D. (1991). A dynamic model of the clarification-thickening process. *Water Res.* 25(10), 1263–1271.
- Verdickt L., Smets I and Van Impe J. F. (2005). Sensitivity analysis of a one-dimensional convection-diffusion model for secondary settling tanks. *Chem. Eng. Comm.* 192, 1567–1585.
- Vitasovic Z. Z. (1989). Continuous settler operation: A dynamic model. In G. G. Patry and D. Chapman, editors, *Dynamic Modelling and Expert Systems in Wastewater Engineering*, pp 59–81. Lewis, Chelsea, MI, USA.

# Centro de Investigación en Ingeniería Matemática (CI<sup>2</sup>MA)

## PRE-PUBLICACIONES 2011

- 2011-03 GABRIEL N. GATICA, ANTONIO MARQUEZ, MANUEL A. SANCHEZ: *Pseudostress-based mixed finite element methods for the Stokes problem in  $R^n$  with Dirichlet boundary conditions. I: A priori error analysis*
- 2011-04 CARLOS D. ACOSTA, RAIMUND BÜRGER: *Difference schemes stabilized by discrete mollification for degenerate parabolic equations in two space dimensions*
- 2011-05 RODOLFO ARAYA, PABLO VENEGAS: *An a posteriori error estimator for an unsteady advection-diffusion problem*
- 2011-06 EDWIN BEHRENS, JOHNNY GUZMAN: *A mixed method for the biharmonic problem based on a system of first-order equations*
- 2011-07 EDWIN BEHRENS, JOHNNY GUZMAN: *A new family of mixed methods for the Reissner-Mindlin plate model based on a system of first-order equations*
- 2011-08 ALFREDO BERMÚDEZ, RAFAEL MUÑOZ-SOLA, CARLOS REALES, RODOLFO RODRÍGUEZ, PILAR SALGADO: *Mathematical and numerical analysis of a transient eddy current problem arising from electromagnetic forming*
- 2011-09 FABIÁN FLORES-BAZÁN, ELVIRA HERNÁNDEZ: *A unified vector optimization problem: complete scalarizations and applications*
- 2011-10 FABIÁN FLORES-BAZÁN, FERNANDO FLORES-BAZÁN, CRISTIAN VERA: *Gordan-type alternative theorems and vector optimization revisited*
- 2011-11 RODOLFO ARAYA, GABRIEL R. BARRENECHEA, ABNER POZA, FREDERIC VALENTIN: *Convergence analysis of a residual local projection finite element method for the Navier-Stokes equations*
- 2011-12 VERONICA ANAYA, MOSTAFA BENDAHMANE, MAURICIO SEPÚLVEDA: *Numerical analysis for HP food chain system with nonlocal and cross diffusion*
- 2011-13 FABIÁN FLORES-BAZÁN, ANTOINE SOUBEYRAN, DINH THE LUC: *Reference-dependent preferences and theory of change*
- 2011-14 RAIMUND BÜRGER, STEFAN DIEHL, SEBASTIAN FARÅS, INGMAR NOPENS: *Simulation of the secondary settling process with reliable numerical methods*

Para obtener copias de las Pre-Publicaciones, escribir o llamar a: DIRECTOR, CENTRO DE INVESTIGACIÓN EN INGENIERÍA MATEMÁTICA, UNIVERSIDAD DE CONCEPCIÓN, CASILLA 160-C, CONCEPCIÓN, CHILE, TEL.: 41-2661324, o bien, visitar la página web del centro: <http://www.ci2ma.udec.cl>



**CENTRO DE INVESTIGACIÓN EN  
INGENIERÍA MATEMÁTICA (CI<sup>2</sup>MA)  
Universidad de Concepción**



Casilla 160-C, Concepción, Chile  
Tel.: 56-41-2661324/2661554/2661316  
<http://www.ci2ma.udec.cl>



---